

Statistical Analysis of Solid Electrolyte Interface Formation: Correlation of Gas Composition, Electrochemical Data and Performance

Sebastian Klick,^{*[a, d]} Karl Martin Graff,^[b, d] Gereon Stahl,^[a, d] Egbert Figgemeier,^[b, c, d] and Dirk Uwe Sauer^[a, c, d]

The SEI is a crucial yet little understood component of lithium-ion batteries. The specific formation processes creating the SEI are still a matter of current research. In our paper, we analyse the electrochemical processes by incremental capacity analysis (ICA) and correlate these results with the evolved gas species and subsequent performance of the cells. 101 cells in total divided in three groups with different electrolytes performed a

formation cycle. Afterwards gas-samples of half of the cells were extracted for analysis. We found a good correlation between variations of gas composition and noticeable ICA-data. Furthermore we explore correlations between formation and initial cell performance after a total of 10 cycles. Our results open new possibilities for a better understanding of formation processes.

Introduction

Lithium-ion batteries have become well-established in many applications from consumer electronics to electric vehicles and large-scale stationary storage systems.

The solid electrolyte interphase (SEI) enables lithium-ion batteries with high energy density by passivating the anode at low potentials.^[1] It is formed during the initial cycles also called formation cycles by reactions on the surface of the anode.^[2–4] These reactions and especially their relations to cell performance are not yet well-understood.^[5] Some review articles summarise the state of the art on the understanding of the SEI.^[3,6]

The SEI consists of organic and inorganic species.^[2,3] The initial SEI evolves during the first cycle(s) (called the formation) of the battery, as the anode is lithiated resulting in potentials below the stability window of commonly used electrolytes.^[3]

Thus, electrolyte reduction leads to the deposition of decomposition products on the active surface of the anode. These products form an initial SEI, which can evolve through subsequent chemical and electrochemical reactions.^[2]

Additives are used to improve the SEI properties and lifetime of lithium ion batteries. Fluoroethylene carbonate (FEC) and vinylene carbonate (VC) can suppress degradation of ethylene carbonate (EC).^[7] VC has been reported to also reduce side reactions at the cathode.^[8] However, larger amounts of VC lead to an increased resistance. This is not the case for increased amounts of FEC.^[8]

The exact mechanism of passivation and the decomposition reaction are subject to current research. For VC several reduction pathways have been reported creating poly(VC), through a partly radical-driven reaction.^[9] CO₂ is generated by decarboxylation of VC.^[9] There is some debate on the reduction pathway of FEC: Defluorination of FEC, resulting in VC and LiF has been proposed,^[2,4,9] while Nie et al.^[7] found poly(FEC) in the FEC-derived SEI.

Gas-Chromatography-Mass-Spectroscopy (GC-MS) has been applied to identify the gas composition after formation.^[10,11] Gas species found after formation include alkanes, ethylene, CO₂, CO and hydrogen.^[10] Cells without film-forming additives such as VC or FEC, release substantial amounts of ethylene.^[12] VC and FEC suppress the reductive decomposition of EC and thus the evolution of ethylene.^[13,14]

Electrical data from first formation cycle have been analysed in various studies.^[15–17] This can yield information on processes during formation^[15,16] or serve as process control mechanism^[17]

The SEI can also be altered by adjusting the conditions during formation cycles.^[10] These conditions also influence the performance of the battery.^[18] Identifying good conditions for SEI formation while keeping the time and cost required for formation low has been the focus of several publications.^[18–20] A faster formation would reduce the required amount and footprint of formation cyclers and thus contribute to cost-savings.

[a] S. Klick, G. Stahl, D. U. Sauer

Chair for Electrochemical Energy Conversion and Storage Systems, Institute for Power Electronics and Electrical Drives (ISEA), RWTH Aachen University, Aachen 52074, Germany
E-mail: Sebastian.Klick@isea.rwth-aachen.de

[b] K. M. Graff, E. Figgemeier

Aging Processes and Lifetime Prediction of Batteries, Institute for Power Electronics and Electrical Drives (ISEA), RWTH Aachen University, 52074 Aachen, Germany

[c] E. Figgemeier, D. U. Sauer

Juelich Aachen Research Alliance, JARA-Energy, Germany

[d] S. Klick, K. M. Graff, G. Stahl, E. Figgemeier, D. U. Sauer

Helmholtz Institute Muenster (HIMS), IEK-12, Forschungszentrum Juelich, Campus-Boulevard 89, 52074 Aachen
E-mail: Sebastian.Klick@gmx.de

 Supporting information for this article is available on the WWW under <https://doi.org/10.1002/batt.202400291>

 © 2024 The Authors. *Batteries & Supercaps* published by Wiley-VCH GmbH. This is an open access article under the terms of the Creative Commons Attribution License, which permits use, distribution and reproduction in any medium, provided the original work is properly cited.

However, the mechanistic understanding of the formation processes is limited at best.^[5] Furthermore formation conditions are a closely guarded trade secret by battery manufacturers limiting systematic mechanistic evaluation of the reactions during formation. Attia et al.^[21] analysed the formation by using carbon black and graphite electrodes with lithium-metal counter electrodes. They demonstrated that the EC reduction occurring above a graphite potential of 0.5 V vs. Lithium does not contribute to the desired passivation.^[21] Thus, they propose fairly high current rates at least during low states of charge during the formation. This is in line with the results of An et al.,^[18] who found that charge throughput at high SOCs is more relevant for the formation of a stable SEI, but in contrast with older publications where higher current rates during formation negatively impact the lifetime of the cell.^[6]

In this paper our aim is to increase the understanding of the formation processes and the influence of different additives on these processes. We explore the question whether the electrical data of the formation process can provide valuable insights to the chemical processes. More specifically we will address the following questions:

- Can differences in reactions within the same configuration of cells be identified based on the electrical data of the formation cycle?
- How do variables from the formation process correlate with performance in terms of capacity and resistance?

These questions require the analysis of a large number of cells as the deviation might only occur in a small number of cells and a sufficient number of cells is required for a sound statistical analysis. The origins of the differences between cells are outside the scope of this work and no intentional defect was added to any cell. A total of 101 cells filled with three different electrolytes were formed and performed 9 cycles followed by a reference performance test (RPT). In addition to the electrical data, we analyse the gas composition of half of the cells after the formation cycle as a proxy for the chemical and electrochemical reactions during the formation process. Correlations between electrical formation data and performance as measured in the RPT are analysed to identify starting points for further research and means for empirical prediction of cell performance based on the formation cycle. In addition, we also analyse correlations between gasses generated during formation. This provides new insights into the respective reactions and their relation.

Experimental and Methodology

101 cells (NMC622|Graphite, 1 Ah) purchased dry from LiFun Technologies are used for these experiments. Cells are cut open and dried in a vacuum drying oven at 40 °C for at least 24 h prior to filling. Cells are then filled with three different electrolyte compositions in a dry room (dew-point below –55 °C) and sealed with a vacuum sealer. The three used electrolyte compositions displayed in Table S1 in the Supporting Information are used as received from Elyte Innovations GmbH, Münster. 28 cells were filled with EC/EMC, without any additives, 36 cell were filled with EC/EMC + 5% FEC and 37 cells were filled with EC/EMC + 5% VC.

Subsequently the cells are kept at 1.5 V for at least 12 h at 25 °C to allow sufficient wetting of the active material. Cells are then clamped between two stainless steel plates with four screws (M3) tightened with a torque of 0.5 Nm for each screw. Cells are then put into an oven at 80 °C. These clamped cells undergo a formation cycle consisting of 8 h storage at constant voltage of 1.5 V, a C/5 constant current charge to 4.2 V, followed by a C/5 discharge to 3.9 V and 8 h rest at open circuit conditions. This formation procedure is performed using a Maccor 4200 testing system. Subsequent cycling and performance tests are performed using Neware BTS 4000 battery cyclers with a current range of up to 6. Cell filling, wetting and formation was done in batches of up to 16 cells at once. Hence, the cells were assembled over a period of three months. Electrolyte was stored in a closed bottle, inside a closed bag in a fridge at ~5 °C.

After formation gas samples are extracted from approximately half of the cells (15 cells without additives, 18 cells with FEC and 18 cells with VC) for analysis (details described below). All cells were degassed and vacuum-sealed to remove the gasses created during formation. Cells perform another 9 cycles in an oven heated to 45 °C at C/5 to stabilise coulombic efficiency and capacity. The performance of all cells was measured with a reference performance test (RPT), consisting of a capacity test at C/2, a quasi Open Circuit Voltage-cycle (qOCV), and pulse tests. The qOCV-test was performed at C/10 for the first 31 cells but then changed to C/20 to further decrease overvoltages, facilitating analysis such as Differential Voltage Analysis (DVA). 16 of these tests stopped prematurely due to a programming error. Hence, these data are not available. For comparison tests performed with C/20 which were terminated correctly are considered. C/10-qOCVs are used to complement these results. The complete RPT is performed in an oven heated to 25 °C. Pulses performed at 70% SOC with a current of 1 A (1 C) were used to calculate a 10 s pulse resistance, by dividing the difference between the voltage prior to the pulse and 10 s after the pulse started by the current of the pulse. After the measurements we identified an issue with the clamps used to connect the pouch-cells to the Neware cyclers used for cycling and the RPT. Due to the thin and narrow tabs amid rather wide clamps, a direct electrical connection between the two contact areas (one used for voltage measurements and one for applying the current) can occur. This effectively means that the measurement is no longer a four-point-measurement. This results in disturbances especially when measuring the resistance using high-current pulses.

This issue increases the measured resistance during the RPT and might also result in slightly lower measured capacities. Due to our large dataset and the fact that we will use a rank-correlation analysis the error might conceal some correlations which could be identified in a data-set with lower errors. Correlations that we identified exist despite the error due to the faulty connection.

Gas Content Analysis

For the gas analysis a gas chromatograph from PerkinElmer (Clarus 690 GC) with a connected mass spectrometer (Clarus SQ8S MS) was used. The system has two columns connected in series. The first column is the Elite-PLOT Q (PerkinElmer) with a length of 30 m and an internal diameter of 0.53 mm. The second is the Elite-GC GS MOLESIEVE (PerkinElmer) column with the same geometry. The latter can be switched in or out of the flow of the GC manually or programmatically. In addition to the MS, the GC also has a TCD (thermal conductivity detector). For the quantitative analysis of the gases, a calibration reference gas mixture from Messer was used. The gas composition is listed in Table S2 in the Supporting Information. The extraction of the gas was carried out in a dry room with a dew-point below –55 °C. The gas was extracted with a gas-

tight syringe (Hamilton). From the gas bag on the side of the cell, approx. 80 gas was extracted and the syringe was then closed. The volume in the syringe was adjusted to exactly 50 and subsequently injected into the GC-MS system.

Incremental Capacity Analysis

Incremental Capacity Analysis (ICA) can be used to identify electrochemical processes in batteries.^[22] It has been applied to identify processes during formation.^[15,16] In this work data were filtered to achieve a smooth ICA-curve. Filtering is focused on smoothing the voltage signal prior to calculating the derivative as suggested in.^[22] A Gauss-Filter is applied on the voltage signal, followed by creating a smoothing spline using `scipy`. The derivative of the spline is calculated. It represents the dV/dQ values. For numerical values as are discussed here, the dQ/dV can simply be calculated by forming the reciprocal.

The filter parameters are kept equal for measurements with the same device and the same current rate in order to exclude effects of the filtering process from influencing any comparison.

Correlation Analysis

The large number of cells investigated here enable a statistical correlation analysis. Correlation does not contain any information about causation.^[23] It implies a connection between the two variables which are strongly correlated. This connection could be a common cause affecting both variables, or some cause-effect relationship between the two variables. In this study we use the spearman correlation (also known as spearman rank-correlation). It is calculated by ranking the variables within the test set and calculating the wider known Pearson correlation coefficient of the ranks.^[24–26] In contrast to the Pearson correlation coefficient, the Spearman one does not test the two variables for linearity but for monotony.^[27] It has also been described as more robust against outliers.^[28] A strictly monotonic dataset would result in a Spearman correlation coefficient of 1 or -1 for increasing, or decreasing monotony, respectively.

Another important parameter when discussing correlations is the p-value.^[26] This essentially gives the probability of observing a distribution under a so called Null-Hypothesis.^[26] Often (and this study is no exception to this) the Null-Hypothesis is that the two parameters in question are not correlated. In this case the p-value gives an estimation of the probability of an observation which is at least as extreme as the observed distribution if the Null-Hypothesis was true.^[26] Different thresholds for significance can be set for p. Correlations with p-values higher than this threshold are not considered significant. In this paper we consider correlations with $p \leq 0.01$ as significant. This means there is a 1% probability of any significant correlation to happen under the Null-Hypothesis, that is without any actual correlation between the variables. The `spearmanr` function of the `scipy.stats` package was used to calculate an estimate for the correlation coefficient. As suggested by the documentation of this function^[29] a permutation test with 30 000 permutations per variable was also performed to validate the results from the numerical approach which only works well for large data-sets. Due to the random sampling of permutations, the obtained p-values are estimates and can differ slightly when trying to reproduce these results. Correlations with p-values below 0.01 in one of the tests are considered significant here.

Results

This section presents the results obtained from our measurements and analyses. We first introduce the results obtained from the formation cycle, including the GC-MS results. This is followed by the results from the reference performance test (RPT). The section ends with a presentation of the identified correlations between features from the initial formation cycle and performance metrics from the RPT.

Formation Cycle

Incremental Capacity Analysis

ICA is applied to the charge phase of the formation cycle. This includes the initial decomposition reactions of additives and solvents.^[16] Figure 1 shows the resulting ICA curves. The three different additives show different features in the low-voltage range as expected.

FEC-containing cells show a peak in the range between 2.46 V and 2.62 V. VC-containing cells show a smaller peak between 2.6 V and 2.68 V. Cells containing no additives show a broader feature stretching from 2.73 V to 2.95 V, with a peak in the range of 2.73 V to 2.8 V as displayed in the inset in Figure 1.

Apart from these initial reactions, the ICA is similar for most cells and no clear differences for the three electrolyte compositions can be seen in Figure 1.

However, two cells (Cell 3 and Cell 23) differ substantially from other cells containing the same electrolyte in terms of the ICA. The IC-curves for these cells are displayed in Figure 2. Cell 3 exhibits a shift of all peaks towards higher voltages, while Cell 23 features an increase of the incremental capacity in the high voltage range. Gas samples of Cells 3 and 23 were also taken and will be presented below.

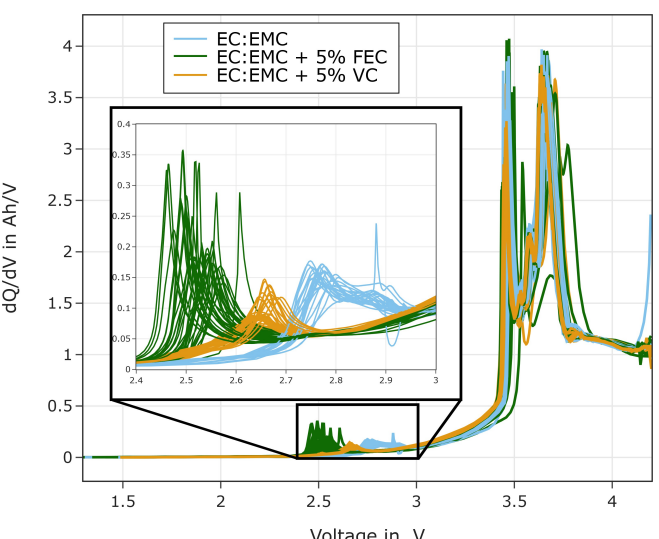


Figure 1. ICA curves of the formation cycle for the cells investigated in this study. The inset shows a magnification of the low-voltage features attributed to initial formation reactions. Cells with different additives show distinct behaviour in this low-voltage region

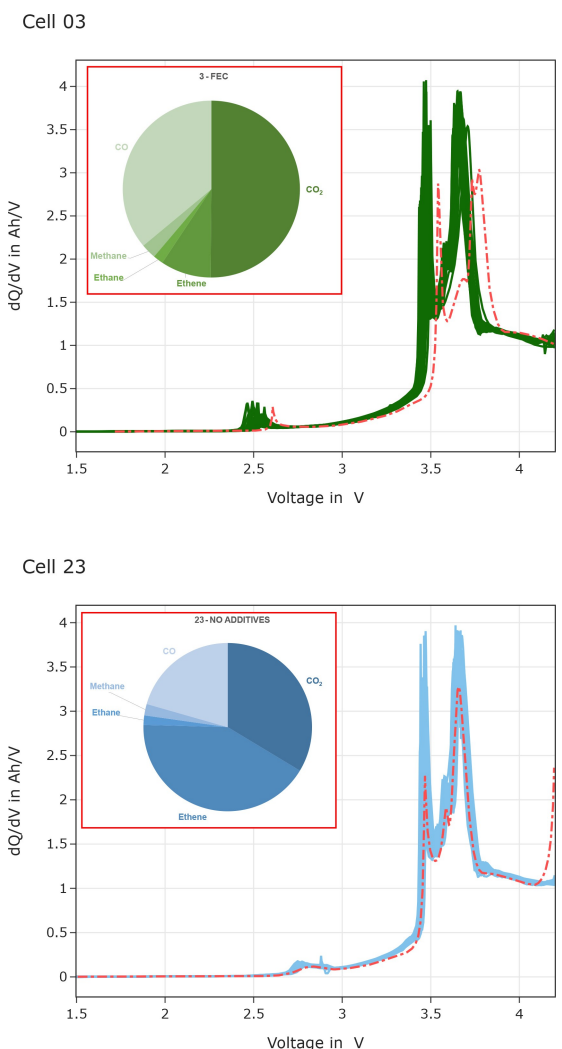


Figure 2. Cells deviating from their respective group. a) Cell 3 (highlighted), and other cells containing FEC, b) Cell 23 (highlighted) and other cells without additives. The inset shows the respective gas composition.

Feature Extraction

Features for the correlation analysis were extracted from the formation cycle. We considered the charge throughput during the constant voltage phase at 1.5 V ($Q_{F,\text{wet}}$), the charge throughput between 1.5 V and 3 V ($Q_{F,LV}$), representing the voltage window that is below the lower operating voltage of the cell, the charge throughput between 3.8 V and 4.2 V ($Q_{F,HV}$), representing the voltage window with minimal changes to the anode potential, and the remaining voltage window between 3 V and 3.8 V ($Q_{F,MV}$). The distribution for the different features is shown in Figure 3. $Q_{F,\text{wet}}$ is lowest for cells containing no additives while VC-containing cells have the highest $Q_{F,\text{wet}}$. Values for $Q_{F,\text{wet}}$ are in the range of 10 mAh approximately 1% of the nominal capacity of the cell. $Q_{F,LV}$ is in the range of 40 mAh. It is lowest for cells containing VC as suggested by the ICA (Figure 1). Cells with FEC have the highest $Q_{F,LV}$. $Q_{F,MV}$ is the major share of the charge throughput with values above 800 mAh for most cells. This feature is highest for cells with VC amid

negligible differences between cells without additives and those with FEC. $Q_{F,HV}$ is in the range around 450 mAh. Cells without additives have a higher median charge throughput in this range, but also a wider spread compared to the other electrolytes. The median for cells with VC is lowest but the range of $Q_{F,HV}$ of these cells is similar compared to cells containing FEC.

Gas Composition

Gas samples were analysed and we calculated the composition of carbon-containing gasses in the samples. This excludes hydrogen which has been reported as a gas species released during formation^[10] as it was not possible to measure it with the GC-MS used. Figure 4 presents the mean distribution for the three different electrolytes.

Gas from cells containing no additives is high in ethylene amid low shares of alkanes and carbonoxides compared to cells with additives. The share of CO is higher for cells with FEC, compared to those with VC.

As mentioned above, the gas compositions in the cells that show deviations in the IC-curves are also different. In Cell 23, a smaller proportion of CO₂ can be seen, while the proportion of ethylene is higher compared to the gas compositions of the cells not deviating in the ICA. In Cell 3, a smaller share of CO₂ can be recognized, while the share of CO is larger, always in relation to the cells not deviating in the ICA. Both gas compositions can be found in Figure 2.

Reference Performance Test

The RPT was conducted after a total of 10 cycles (including the formation cycle). It consists of a capacity test at C/2, a low-current quasi-OCV cycle, and pulse tests.

Capacity

Figure 5 shows the capacity distribution for the cells with respect to the electrolyte. While the distribution is similar for all cells, the maximum, minimum and mean capacities of cells containing VC are lower compared to cells with FEC and those without additives. The difference is stronger for C/20 cycles shown in Figure 5. In this case cells containing VC have the lowest capacity while cells with FEC and those without additives still perform similarly. Cells without additives exhibit a larger spread of capacities.

Resistance

Two resistance-related values were analysed: the 10 s pulse resistance and the difference between the average charge and discharge voltage of the capacity test. Both are in good agreement for most cells as shown in Figure 6. At pulse

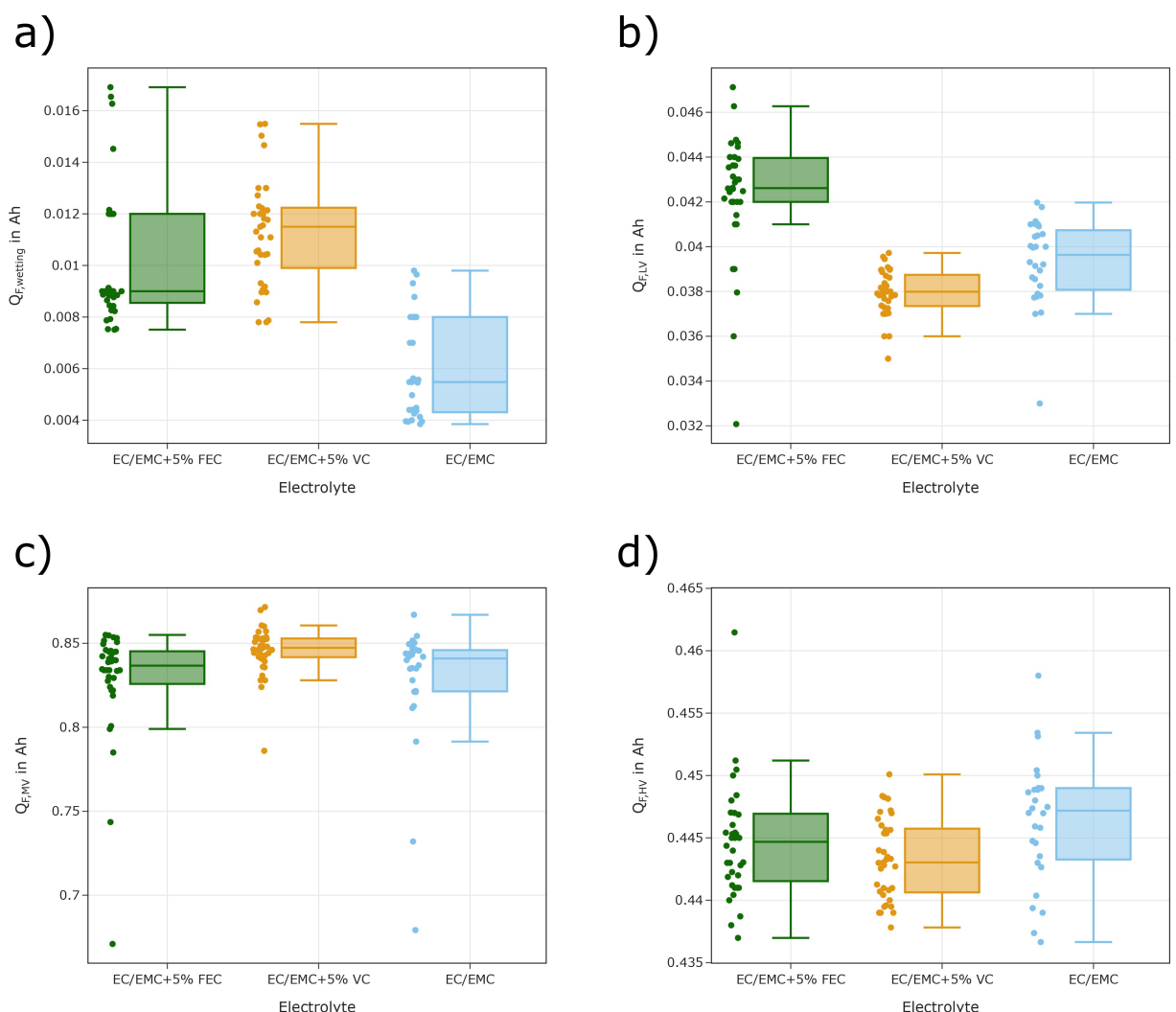


Figure 3. Boxplots displaying the distribution of features extracted from the formation cycle. a) $Q_{F,wet}$, the charge throughput at 1.5 V, b) $Q_{F,LV}$, the charge throughput between 1.5 V and 3 V, c) $Q_{F,MV}$, the charge throughput between 3 V and 3.8 V, d) $Q_{F,HV}$, the charge throughput between 3.8 V and 4.2 V.

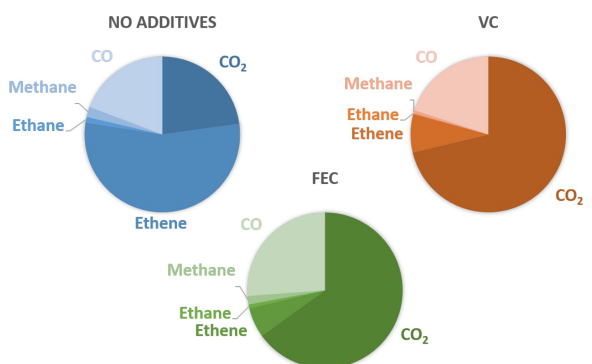


Figure 4. Comparison of the share of carbon-containing gases of the gas samples taken after formation with different electrolyte additives.

resistances above 0.2Ω cells do not follow the linear relationship, which is observable for lower resistances. Cells containing FEC and no additives follow the same linear relationship, while cells with VC exhibit higher overvoltages even at comparable pulse resistance values. Additionally, the overall trend shows

that both overvoltages and pulse resistance is higher for cells containing VC.

Low Current Cycling Results

Based on the low current (C/10 for the first 31 cells, and C/20 for subsequent cells), both DVA and ICA are calculated. The DVA displayed in Figure S2 in the Supporting Information shows little differences between cells containing FEC and no additives. The cells containing VC differ from the other cells. The peak indicating the transition between the graphite plateaus is wider and reduced in height during the charge process. A similar observation can be made during the discharge. Figure 7 shows exemplary DVA-curves of 6 different cells recorded with different current rates (C/10 and C/20). An increased current reduces the height of the peak amid a peak-broadening for cells containing FEC and those without additives. There is very little difference in terms of the peak-shape between the two cells containing VC.

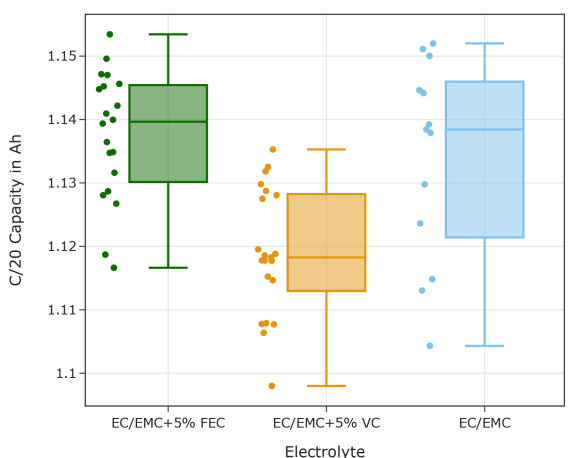
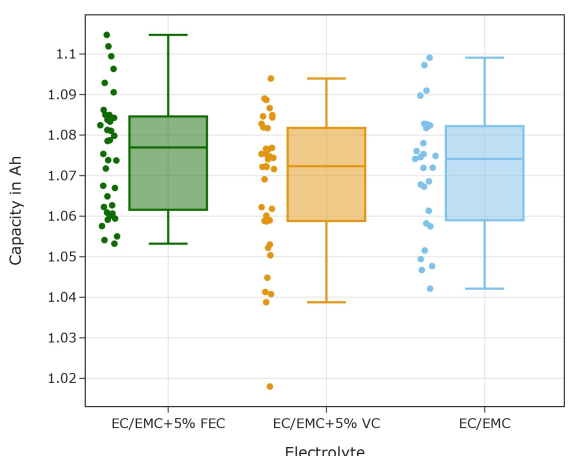


Figure 5. Capacities as measured during the RPT. a) C/2 capacity: Cells containing VC show slightly lower C/2 capacities, while FEC-containing cells perform best b) C/20 capacity; the difference between the three groups increases as VC-containing cells demonstrate lower capacities. Capacities as measured during the RPT. a) C/2 capacity: Cells containing VC show slightly lower C/2 capacities, while FEC-containing cells perform best b) C/20 capacity; the difference between the three groups increases as VC-containing cells demonstrate lower capacities.

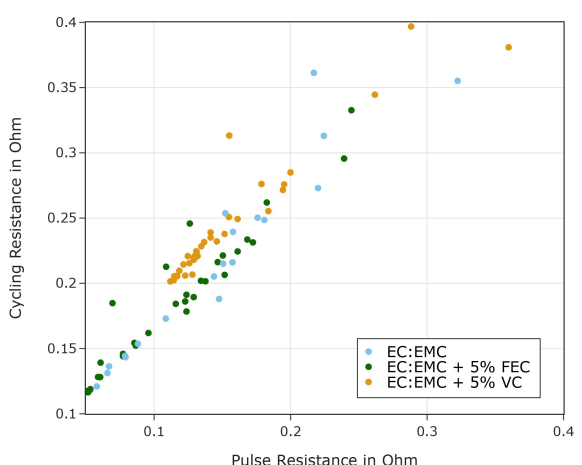


Figure 6. Cycling resistance over pulse-resistance for the three investigated electrolytes. Cycling resistance is calculated based on the C/2 capacity test, pulse resistance is obtained from a 10 s charge pulse with 1 C at 70% SOC.

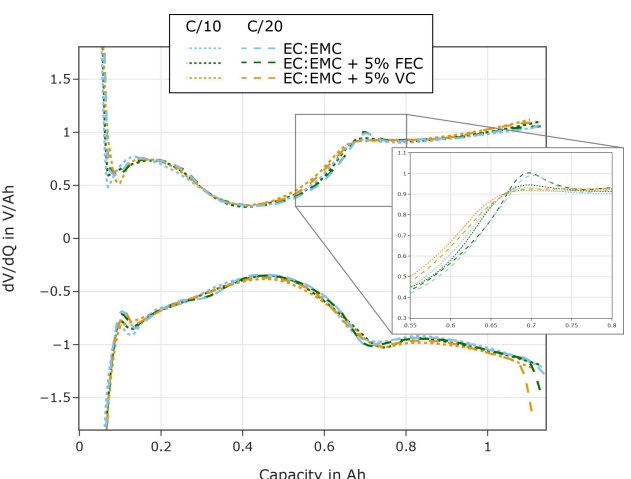


Figure 7. Exemplary DV-curves of six different cells obtained from a C/10 cycle (dotted) and a C/20 cycle (dashed).

ICA complements the results obtained from the DVA. In this case the first peak of the ICA-curve is slightly shifted to higher voltages for cells containing VC. This is not the case for the second peak as shown in Figure 8. Cells which underwent the qOCV with a higher current of C/10 also show broader peaks and a shifted peak of the ICA during charge as shown in Figure S3 in the Supporting Information.

For the C/20 test a decreased absolute incremental capacity at the beginning of the discharge process is detectable at high voltages in the discharge IC-curve. A comparison of the IC-values at the beginning of the discharge process is shown in Figure 9. VC cells exhibit the lowest absolute incremental capacity at the beginning of the discharge phase. This effect is not observed for cells cycled with C/10 (Figure S1 in the Supporting Information).

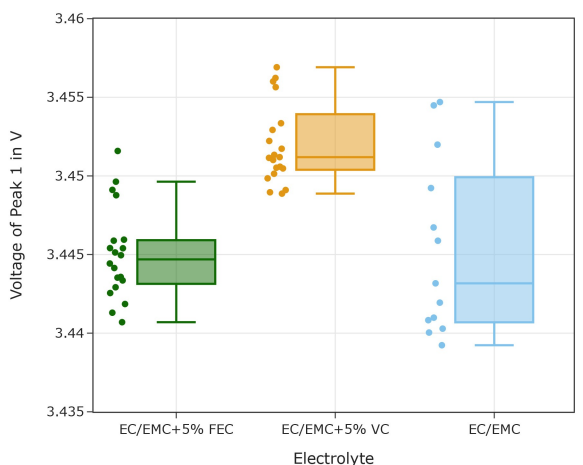
Correlation Analysis

The large data-set enables statistical correlation analysis. The spearman correlation coefficient is used due to its capability to identify non-linear correlations and its robustness against outliers.^[28] p-values are calculated by permutation.^[30,31] The significance threshold was set to 0.01. Hence, correlations with p-values above 0.01 will not be considered as significant here. To decouple the effects of the electrolyte on the cells performance, correlations were analysed for each group of cells individually.

Predictive Correlations

Correlations between features of the first formation cycle and later performance can support cell-grading and early sorting of cells. The features from the formation cycle analysed here are explained in Table 1. These features are obtained from the first formation cycle, including the coulombic efficiency. The correlation of these features with the capacity, the pulse

a)



b)

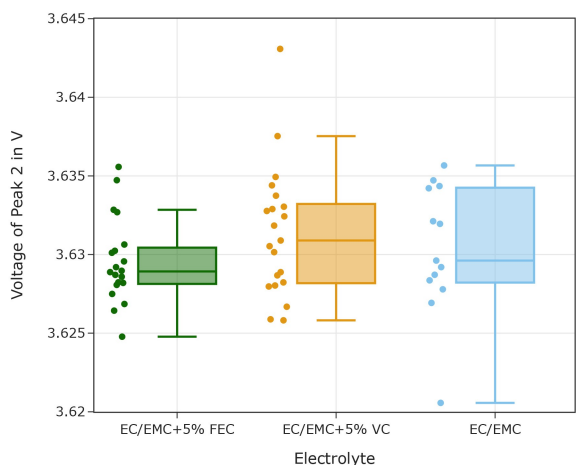


Figure 8. Distribution of voltages corresponding to the first (a) and second (b) peak in the I-V.

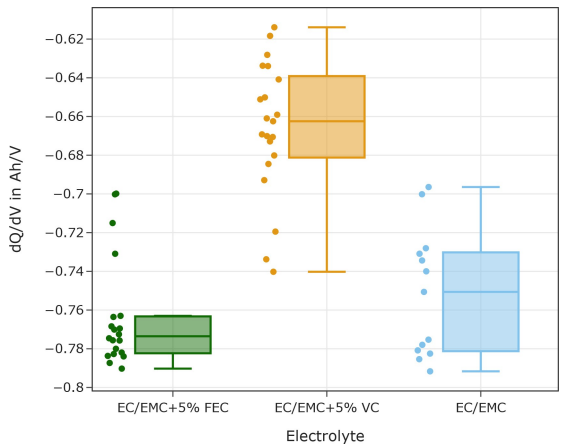


Figure 9. Distribution of the initial incremental capacity values at the beginning of the discharge process. A clear difference between VC and the other electrolytes is visible.

Table 1. Features for correlation analysis obtained from the first formation cycle.	
Symbol	Description
$Q_{F,Cha}$	Charge during Formation Cycle
V_F	Mean Charging Voltage during Formation
$Q_{F,LV}$	Charge Throughput between 1.5 & 3 V
$Q_{F,HV}$	Charge Throughput between 3.8 & 4.2 V
$Q_{F,MV}$	Charge Throughput between 3 & 3.8 V
$Q_{F,Dch}$	Discharge Capacity at first discharge
$Q_{F,CL}$	$Q_{F,Cha} - Q_{F,Dch}$
CE_F	$\frac{Q_{F,Dch}}{Q_{F,Cha}}$
$Q_{F,wet}$	Charge throughput at 1.5 V

resistance, the cycling resistance (Cyc Resistance) as explained above and the loss of capacity between the discharge after formation and the capacity measured during the RPT (Q_{loss}) was

calculated for each subset of cells containing the same electrolyte.

The significant correlations ($p \leq 0.01$) are marked with bold and white correlations coefficients in Figure 10.

For cells without additives a significant negative correlation between $Q_{F,wet}$ and performance in the RPT exists. Higher $Q_{F,wet}$ correlates with reduced capacity and increased resistance during the RPT, as well as increased Q_{loss} . Furthermore, Q_{loss} is negatively correlated with $V_{F,Cha}$ amid positive correlations with $Q_{F,Char}$, $Q_{F,MV}$, $Q_{F,Dch}$. There is also a significant positive correlation between the capacity and $Q_{F,HV}$.

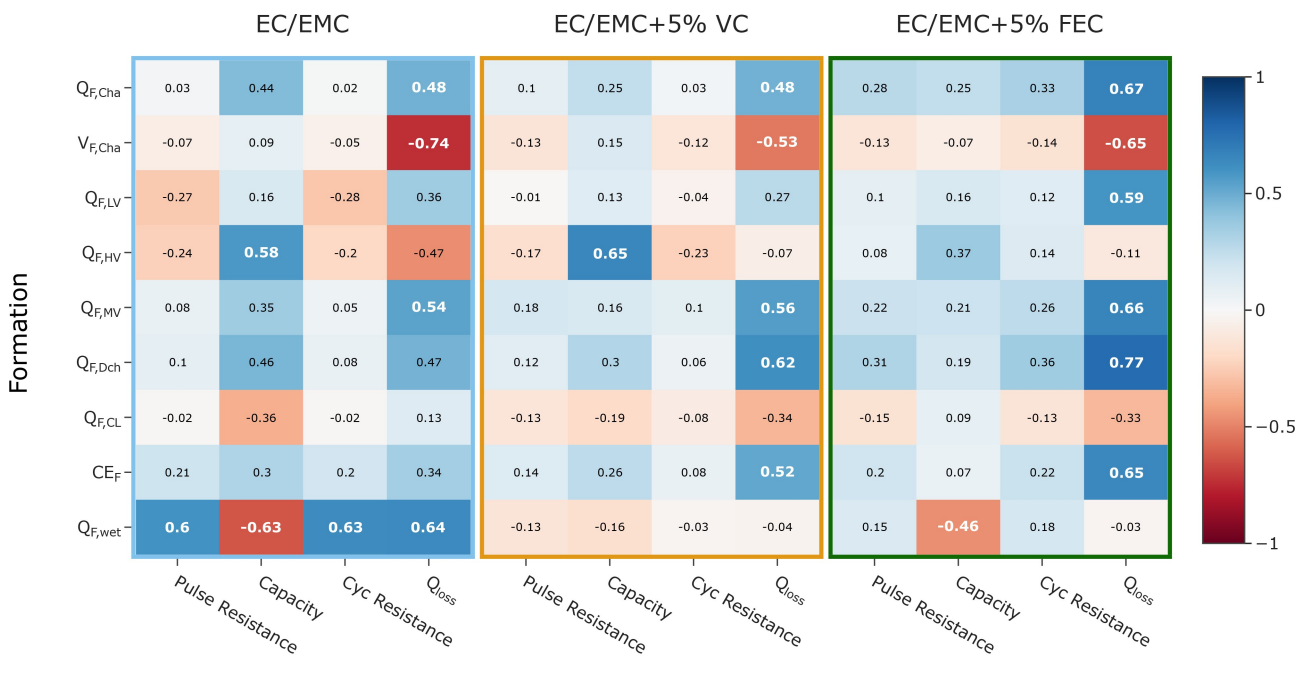
This correlation between capacity and $Q_{F,HV}$ is also found for cells containing VC. Apart from this one correlation between a formation feature and the performance, we did not identify any other significant direct correlation between performance and formation features. However, Q_{loss} shows significant positive correlations with, $Q_{F,Char}$, $Q_{F,LV}$, $Q_{F,MV}$, $Q_{F,Dch}$ and the coulombic efficiency CE_F , while being negatively correlated with $V_{F,Cha}$. In contrast to cells without additives $Q_{F,wet}$ exhibits no significant correlation with any of the analysed parameters.

For cells containing FEC, the correlation between $Q_{F,HV}$ and the capacity observed in both other groups is weaker and not significant. A negative correlation between Capacity and $Q_{F,wet}$ is the only significant direct correlation between performance parameters and the formation features. Q_{loss} is positively correlated with $Q_{F,Char}$, $Q_{F,LV}$, $Q_{F,MV}$, $Q_{F,Dch}$ and CE_F , amid a negative correlation with $V_{F,Cha}$.

Gas Correlations

Correlating the gas composition with features of electrical data from the formation cycle, and other gasses provides a statistical approach to identify processes which are correlated, and those that are independent.

In this section we focus on the charge throughput in different parts of the formation process: $Q_{F,wet}$, $Q_{F,LV}$, $Q_{F,MV}$, $Q_{F,HV}$,



Reference Performance Test

Figure 10. Correlation coefficients between features of the formation cycle and performance during the RPT. Numbers specify the correlation coefficient. Bold, white numbers indicate significant correlations ($p \leq 0.01$). Sample size n is 28, 36, and 37 for cells with EC/EMC, EC/EMC + 5% VC, and EC/EMC + 5% FEC respectively.

and the gasses that were measured. We also considered the total amount of carbon-containing formation gasses, and nitrogen and oxygen. The formation gasses were normalised to the total formation gasses measured, while nitrogen and oxygen values are used without any normalisation. We expect a strong positive correlation for oxygen and nitrogen.

Figure 11 shows the correlations for the three cell groups. White bold numbers indicate significant correlations. For cells without additives, a significant and strong negative correlation between the share of CO_2 and ethylene exists. Furthermore, a positive correlation between air (nitrogen and oxygen) and CO

was found. Regarding the electrical data, a significant negative correlation was found between the $Q_{F,wet}$ and ethylene.

For cells containing VC, no significant correlation between the considered formation features and gasses are observed. However, strong and significant correlations between gasses are identified. CO_2 is negatively correlated with all other formation gasses (CO, ethylene, ethane, and methane). These other gasses are in turn strongly correlated with each other. A significant correlation between oxygen and the methane share is also found.

For cells with FEC, significant correlations between $Q_{F,wet}$ and alkanes (methane and ethane) exist. This correlation is positive

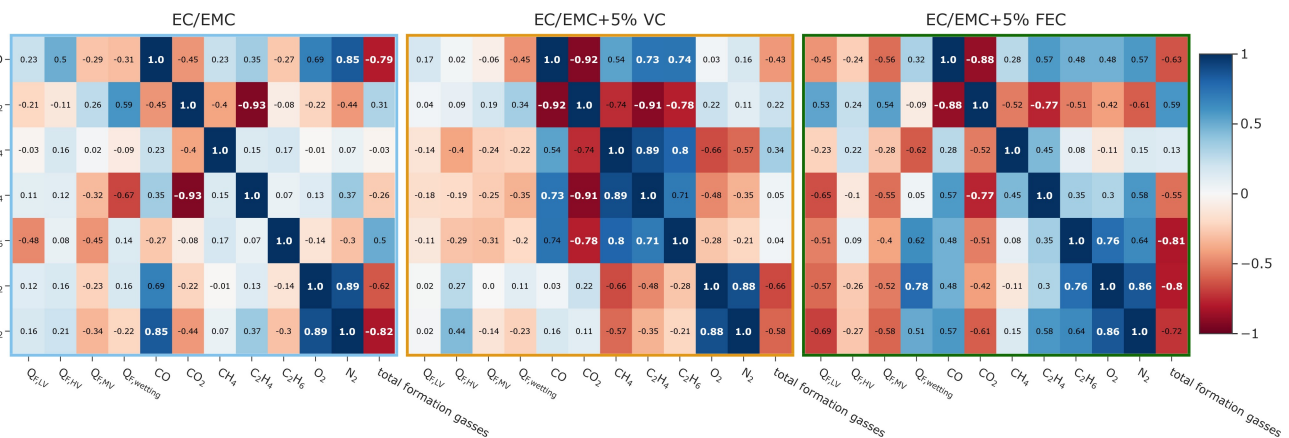


Figure 11. Correlations between gasses, and electrical parameters. Numbers specify the correlation coefficient. Bold, white numbers indicate a significant correlations ($p \leq 0.01$). Sample size n is 15, 18, and 18 for cells with EC/EMC, EC/EMC + 5% VC, and EC/EMC + 5% FEC respectively.

in case of methane and negative in case of ethane. $Q_{F,LV}$ is significantly negatively correlated with ethylene and nitrogen. In terms of the correlation between gasses, CO_2 is significantly negatively correlated with CO, ethylene and nitrogen. Significant positive correlations exist between ethane, nitrogen and oxygen.

Discussion

Formation

The results obtained from the formation cycle are in good agreement with previous studies, which suggest the order of decomposition potentials to be FEC > VC > EC.^[14] This fits well with the observed peaks in the formation ICA. The high share of ethylene in cells without additives supports a reductive decomposition of EC as proposed in several publications.^[32,33] The higher share of CO and CO_2 for cells containing additives indicate effective suppression of EC-decomposition, in line with results from other studies.^[12–14,34]

Reference Performance Test

The results of the reference performance test indicate, that cells containing 5% VC suffer from substantial kinetic limitations. Higher impedances for cells containing VC have been observed and were expected.^[35] In agreement with the literature,^[35] the resistance and overvoltages are higher, compared to the other cells. Even when considering cells which have a similar 10 s pulse resistance, overvoltages during the C/2 capacity test are higher compared to other cells. This indicates a limiting process with a time-constant above 10 s.

The reduced peak height amid a wider peak for the C/20 DVA of cells containing VC also points at kinetic limitations. The fact, that other cells show a similar behaviour, when tested with a current rate of C/10 supports this finding. However, no major difference for cells containing VC has been identified between the two current rates.

In addition the shift of the first IC-peak to higher voltages observed for cells containing VC can also be explained by rather slow transient processes at the beginning of the charge process. As it takes more than 1 hour for the cells to reach the voltage of this first IC-peak, this would require very slow processes. As the cells only differ in terms of the additives, these time constants should be related to the SEI or the electrolyte.

Interestingly little difference is found between cells containing FEC and those without any additives, indicating similar kinetics for the intercalation process at the anode.

Correlations

A higher mean voltage during formation is correlated with reduced losses in subsequent cycles for all cell groups. The charge throughput in the upper voltage window (3.8–4.2 V,

referred to as $Q_{F,HV}$) is also positively correlated with the capacity for cells without additives and those with VC. This correlation is weaker and not significant for cells containing FEC. These correlations support the findings by An et al.^[18] that shallow cycling at high voltages improved capacity retention. They used EC:DEC electrolyte, without additives. However, the increased $Q_{F,HV}$ is not significantly correlated with capacity during the RPT in the case of FEC. One explanation is, that FEC is also decomposed at the cathode at high SOCs resulting in additional charge throughput at high cathode (and thus cell) potentials. Indeed, we observed a higher $Q_{F,HV}$ for cells containing FEC compared to those with VC. However, $Q_{F,HV}$ for cells without additives is even higher than for cells containing FEC (see Figure 3). Kim et al.^[36] found that FEC can also negatively affect cell performance due to side reactions at cathodes with a low degree of lithiation at elevated temperatures. As formation cycling was performed at 80 °C, this provides a possible explanation of the correlation we found: higher charge throughput at high voltages is correlated with an increased capacity, but in the presence of FEC, side-reactions negatively affect the capacity partly overlay this effect.

The correlation of $Q_{F,wet}$ with all performance features in case of cells without additives and the capacity in the case of cells containing FEC is more difficult to relate to known processes. So far the wetting process has received little attention with regard to the charge throughput at the low voltages applied to avoid copper corrosion.^[20] Our results indicate a connection between charge throughput during wetting and later performance for cells without additives but more research is required to analyse the nature of this connection.

Regarding the correlations between gasses, we identified very strong and significant correlations between almost all gasses related to formation processes for cells containing VC. This indicates a strong connection between the processes causing the gas evolution. Based on the correlation pattern the process causing the evolution of CO_2 is competing with other processes causing the evolution of CO, ethylene and alkanes. This is in line with investigations of reductive VC-decomposition showing that decarboxylation of VC leads to the release of CO_2 .^[9] The resulting SEI effectively suppresses the evolution of the other formation-related gasses (alkanes, CO and ethylene).^[34]

For FEC, the suppression of reactions yielding CO and ethylene is also observed by a strong negative correlation between CO_2 and the two gasses. This is in line with publications suggesting the evolution of CO_2 from FEC reduction.^[9,37] However, alkanes exhibit less significant and weaker negative correlations with CO_2 compared to cells with VC. This indicates a weaker connection between the release of alkanes and the evolution of CO_2 .

Cells without additives show just one correlation between gas species: CO_2 is negatively correlated with ethylene. Following the line of argument, this would mean a process releasing CO_2 that competes with or prevents the evolution of ethylene or vice versa. Schwenke et al.^[12] showed that CO_2 leads to a reduction in typical degradation products such as ethylene.

To the best of our knowledge no reduction reaction for EC or EMC yielding stable SEI components and CO₂ has been reported. Possible sources of CO₂ in these cells are lithium carbonate traces on the cathode surface,^[38] or products of EC-oxidation reactions on the cathode surface.^[39] Further research is required to identify the connection between CO₂ and ethylene in this case.

Conclusions

In this paper we analysed gassing and electrochemical data of the formation cycle as well as performance after a total of 10 cycles including the formation cycle for cells containing three different electrolytes with the aim to identify correlations between first-cycle features and performance in terms of capacity and impedance. In addition, we investigated whether deviations in terms of the gas composition could also be detected by the electrical measurements.

Indeed, differences between the additives are easily identifiable in the electrical data of the formation cycle as well as the gas composition. In addition, strong anomalies in the electrical data coincide with a different gas composition. Thus, analysing electrical data can support process control during formation. By analysing the correlation of parameters gathered during the initial formation cycle and later performance tests we conclude that some metrics such as initial coulombic of the formation cycle or the initial capacity, which was used in^[10] to compare the performance of cells with different C-rates during formation have limited merits for predicting capacity, especially when FEC is used. Rather, our data suggest that a high loss of lithium-ions in the initial cycle is offset by lower losses in the subsequent cycles.

However, some correlations which can be applied to estimate cell performance were identified. We found a moderate to strong correlation between charge throughput during the upper voltage window (3.8 V–4.2 V) and capacity during the RPT for cells containing VC or no additives. This is in line with findings by An et al.,^[18] that cycling in the upper voltage window during formation is beneficial for the cell lifetime. For cells without any additives the charge throughput during the 8 h wetting period correlates strongly with all performance parameters obtained from the RPT; a higher charge throughput during wetting correlates with higher resistance and lower capacity.

Further research is required to probe whether some of these correlations are connected by a direct cause-effect-relationship, or whether both parameters depend on an unknown third parameter. If cause-effect relationships can be found by future research, formation protocols could be systematically improved. The identification of gassing- and SEI-forming processes can also contribute to a systematic development of formation protocols, avoiding unwanted side reactions while improving conditions for desired ones. Further research into the identification of these processes is ongoing and will be reported in the future. Furthermore, an ageing study using cells mentioned here is on-going and enables the correlation from differences

during formation with differences in the degradation of the batteries.

Our dataset can be used to advance machine learning or AI-based models for predicting formation quality. We are collaborating with colleagues more experienced in the field of AI for battery applications to investigate this in more detail. Furthermore the data of the RPT and formation cycle as well as GC-MS data is available under DOI 10.18154/RWTH-2024-06739, to facilitate modelling, machine learning and AI applications.

Regarding the influence of additives on cell-performance we identified very slow processes affecting cells containing 5% VC. They exhibit a higher overvoltage and resistance compared to cells containing FEC and those without additives. Furthermore VC-containing cells exhibit clearly detectable kinetic limitations at current rates as low as C/20. Further research elucidating the cause of these slow kinetics could provide valuable insights for SEI design.

Our research demonstrates that a basic connection between gassing and the ICA of the formation cycle exists: outliers identified by the ICA also show a deviation in terms of the gas composition. A systematic correlation analysis provides new starting points for future research: the surprisingly strong correlation between high voltage charge throughput during formation, and capacity in the performance test, a weak (or non-existing) correlation between coulombic losses during formation and capacity in the performance test, and the differences between the three electrolytes all ask for further research.

Acknowledgements

We gratefully acknowledge the funding of this work by BMBF under the projects E-FloA (Funding Code 03XP0349A) and BatGasMod (Funding Code 03XP0311B). We like to thank Syrine Frini and Gizem Simsek for their support in the laboratory regarding gas sampling and cell filling. Open Access funding enabled and organized by Projekt DEAL.

Conflict of Interests

The authors have not conflict of interest to declare.

Data Availability Statement

To facilitate further analysis of the data, we released raw data from both the formation cycle as well as the RPT together with GC-MS raw data. They are publicly available under DOI 10.18154/RWTH-2024-06739. Additional data can be obtained from the authors upon reasonable request.

Keywords: Lithium-ion battery · Formation · SEI · Gassing · Battery Grading

- [1] E. Peled, *J. Electrochem. Soc.* **1979**, *126*, 2047.
- [2] S. K. Heiskanen, J. Kim, B. L. Lucht, *Joule* **2019**, *3*, 2322.
- [3] S. J. An, J. Li, C. Daniel, D. Mohanty, S. Nagpure, D. L. Wood, *Carbon* **2016**, *105*, 52.
- [4] Y. Wang, Y. Liu, Y. Tu, Q. Wang, *J. Phys. Chem. C* **2020**, *124*, 9099.
- [5] H. Adenusi, G. A. Chass, S. Passerini, K. V. Tian, G. Chen, *Adv. Energy Mater.* **2023**, *13*, 2203307.
- [6] V. A. Agubra, J. W. Fergus, *J. Power Sources* **2014**, *268*, 153.
- [7] M. Nie, J. Demeaux, B. T. Young, D. R. Heskett, Y. Chen, A. Bose, J. C. Woicik, B. L. Lucht, *J. Electrochem. Soc.* **2015**, *162*, A7008.
- [8] D. Y. Wang, N. N. Sinha, J. C. Burns, C. P. Aiken, R. Petibon, J. R. Dahn, *J. Electrochem. Soc.* **2014**, *161*, A467.
- [9] A. L. Michan, B. S. Parimalam, M. Leskes, R. N. Kerber, T. Yoon, C. P. Grey, B. L. Lucht, *Chemistry of Materials* **2016**, *28*, 8149.
- [10] M. Leißing, F. Horsthemke, S. Wiemers-Meyer, M. Winter, P. Niehoff, S. Nowak, *Batteries & Supercaps* **2021**, *4*, 1344.
- [11] L. Geng, D. L. Wood, S. A. Lewis, R. M. Connatser, M. Li, C. J. Jafta, I. Belharouak, *J. Power Sources* **2020**, *466*, 228211.
- [12] K. U. Schwenke, S. Solchenbach, J. Demeaux, B. L. Lucht, H. A. Gasteiger, *J. Electrochem. Soc.* **2019**, *166*, A2035.
- [13] B. Zhang, M. Metzger, S. Solchenbach, M. Payne, S. Meini, H. A. Gasteiger, A. Garsuch, B. L. Lucht, *J. Phys. Chem. C* **2015**, *119*, 11337.
- [14] S. A. Delp, O. Borodin, M. Olguin, C. G. Eisner, J. L. Allen, T. R. Jow, *Electrochim. Acta* **2016**, *209*, 498.
- [15] J. C. Burns, R. Petibon, K. J. Nelson, N. N. Sinha, A. Kassam, B. M. Way, J. R. Dahn, *J. Electrochem. Soc.* **2013**, *160*, A1668.
- [16] S. Theil, *Elektrolytalterung in Lithium-Ionen-Batterien*, Ph.D. thesis, Universität Ulm **2016**.
- [17] A. Weng, J. B. Siegel, A. Stefanopoulou, *Front. Energy Res.* **2023**, *11*.
- [18] S. J. An, J. Li, Z. Du, C. Daniel, D. L. Wood, *J. Power Sources* **2017**, *342*, 846.
- [19] R. Drees, F. Lienesch, M. Kurrat, *J. Energy Storage* **2021**, *36*, 102345.
- [20] C. Mao, S. J. An, H. M. Meyer, J. Li, M. Wood, R. E. Ruther, D. L. Wood, *J. Power Sources* **2018**, *402*, 107.
- [21] P. M. Attia, S. J. Harris, W. C. Chueh, *J. Electrochem. Soc.* **2021**, *168*, 050543.
- [22] M. Dubarry, D. Anseán, *Front. Energy Res.* **2022**, *10*, 1023555.
- [23] N. Gogtay, U. Thatte, *The Journal of the Association of Physicians of India* **2017**, *65*, 78–81.
- [24] B. Mirkin, Learning Correlations, in B. Mirkin (Editor), *Core Data Analysis: Summarization, Correlation, and Visualization*, pages 163–292, Springer International Publishing, Cham **2019**.
- [25] J. Hauke, T. Kosowski, *QUAGEO* **2011**, *30*, 87.
- [26] C. Xiao, J. Ye, R. M. Esteves, C. Rong, *Concurrency and Computation: Practice and Experience* **2016**, *28*, 3866.
- [27] K. H. Zou, K. Tuncali, S. G. Silverman, *Radiology* **2003**, *227*, 617.
- [28] J. C. Caruso, N. Cliff, *Educ. Psychol. Meas.* **1997**, *57*, 637.
- [29] ScipyStats.Spearmanr – SciPy v1.13.0 Manual, <https://docs.scipy.org/doc/scipy/reference/generated/scipy.stats.spearmanr.html>.
- [30] M. D. Ernst, *Statistical Science* **2004**, *19*, 676.
- [31] B. Phipson, G. K. Smyth, *Stat. Appl. Genet. Mol. Biol.* **2010**, *9*.
- [32] N. Laszcynski, S. Solchenbach, H. A. Gasteiger, B. L. Lucht, *J. Electrochem. Soc.* **2019**, *166*, A1853.
- [33] M. Metzger, B. Strehle, S. Solchenbach, H. A. Gasteiger, *J. Electrochem. Soc.* **2016**, *163*, A798.
- [34] H. Ota, Y. Sakata, A. Inoue, S. Yamaguchi, *J. Electrochem. Soc.* **2004**, *151*, A1659.
- [35] J. C. Burns, R. Petibon, K. J. Nelson, N. N. Sinha, A. Kassam, B. M. Way, J. R. Dahn, *J. Electrochem. Soc.* **2013**, *160*, A1668.
- [36] K. Kim, I. Park, S.-Y. Ha, Y. Kim, M.-H. Woo, M.-H. Jeong, W. C. Shin, M. Ue, S. Y. Hong, N.-S. Choi, *Electrochim. Acta* **2017**, *225*, 358.
- [37] N. N. Intan, J. Pfaendtner, *ACS Appl. Mater. Interfaces* **2021**, *13*, 8169.
- [38] S. E. Renfrew, B. D. McCloskey, *ACS Appl. Energ. Mater.* **2019**, *2*, 3762.
- [39] B. L. D. Rinkel, D. S. Hall, I. Temprano, C. P. Grey, *J. Am. Chem. Soc.* **2020**, *142*, 15058.

Manuscript received: April 29, 2024

Revised manuscript received: July 18, 2024

Accepted manuscript online: July 26, 2024

Version of record online: September 13, 2024